Novel Fuel Production Based on Sonochemistry and Sonoelectrochemistry

Md. Hujjatul Islam[a], J. J. Lamb[a & b], K. M. Lien[a], O. S. Burheim[a], J-Y. Hihn[c], B. G. Pollet[a]

[a] Department of Energy and Process Engineering, Hydrogen Energy and Sonochemistry Group & ENERSENSE, NTNU, Trondheim, Norway
[b] Department of Electronic Systems & ENERSENSE, NTNU, Trondheim, Norway
[c] Institut UTINAM, University of Franche-Comte, Besancon, France

Sonochemistry has been used in many applications where it is employed to improve both catalytic and synthetic processes; whereas, sonoelectrochemistry has been used in various studies including organic syntheses, environmental (soil and water) treatments, water disinfection and various analytical procedures. In the ongoing energy transition from a fossil-based energy economy, society requires energy forms that can be readily stored and transported. This can be achieved using rechargeable batteries, biofuels and hydrogen. Hydrogen (H_2) is an attractive fuel source due to its rather high specific energy compared to other conventional fuels. Power ultrasound could be an attractive alternative since the ultrasonication of water produces H_2. Alternatively, biogas production could be another fuel source. However, lignocellulose presents a bottleneck due to its rigid and obstinate structure. Power ultrasound could be adopted as a pretreatment of lignocellulosic materials to improve their utilisation in the production of biogas.

Introduction

Power ultrasound has been used in many applications such as the chemical and processing industries where it is employed to improve both catalytic and synthetic processes and to produce new chemicals. This technology area has been termed sonochemistry, which mainly focusses on chemical reactions in solutions yielding an increase in erosion of catalytic surfaces, reaction kinetics, and product yield (1). Sonoelectrochemistry is the study of the combination of ultrasound and electrochemical processes and its applications (1–3). This area of research covers various studies from organic syntheses, polymeric materials syntheses, production of nanomaterials, environmental (soil and water) treatments, water disinfection, corrosion of metals, analytical procedures, film and membrane preparations to the elucidation of electrochemical mechanisms in various ‘exotic’ solvents.

In the ongoing energy transition in our society from a fossil-based to a renewable energy economy, most of the energy input will change from readily storable carbons and hydrocarbons into intermittent electricity (4). This means that we need to process electricity efficiently and intensively into forms that can be stored and transported. Such a mix is likely to be presented by chargeable batteries, hydrogen (H_2) systems and biofuels. Power ultrasound is a tool that can allow for more intensive and more efficient ways for the energy conversion required in this transition, and here we look particularly on efforts within the production of H_2 and biofuels.

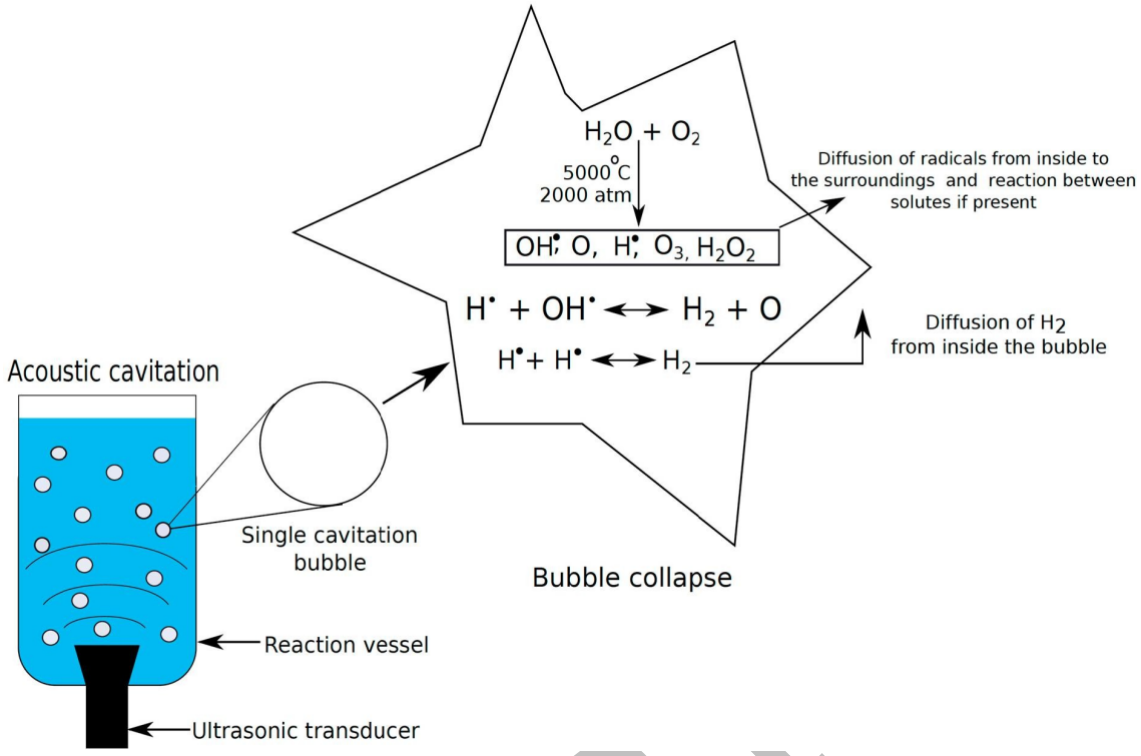

Figure 1. Schematic representation of hydrogen production through water sonolysis (3)

H_2 is an attractive fuel source due to its rather high specific energy compared to other conventional fuel. There are various methods available to produce H_2 such as thermal, electrolytic, photocatalytic and biological methods. In the thermal process, H_2 is produced from fossil fuel and biomass through reforming and gasification process. H_2 can also be produced through the electrolytic splitting of water into H_2 and O_2 using external energy source. Currently, around 50% of total hydrogen demand comes from natural gas reforming, 30% from oil reforming, 18% from coal gasification, and only 3.9% comes from water electrolysis. This means that more than 90% of the total hydrogen demand comes from fossil fuel. However, production of hydrogen from fossil resources is an environmentally unfriendly method since they release large amounts of fossil CO_2 (up to 10 kg of CO_2 per kg of H_2 production depending on the types of raw materials and processing method). H_2 production through sonochemical and sonoelectrochemical method could be an attractive alternative. The sonochemical production of hydrogen involves the use of power ultrasound to breakdown water molecules into OH• and H• radicals, where the recombination of these radicals produces H_2 (Figure 1).

Moreover, the use of ultrasound in water electrolysis enhances hydrogen production. Sonochemical hydrogen production is entirely radical-dependent. There are two reaction mechanisms that are involved in sonochemical hydrogen production (3).

$$H\bullet + OH\bullet \rightleftarrows H_2 + O \quad [1]$$

$$H\bullet + H\bullet \rightleftarrows H_2 \quad [2]$$

Reaction 1 takes place inside the collapsing bubble, which is also called the gas phase reaction. Reaction 2 takes place at the bubble wall. Merouani *et al.* (5) proposed that 99.9% of hydrogen is produced by the gas phase reaction (Reaction 1), whereas the recombination reaction of H• plays a minor role. Among all the radicals formed by water

sonolysis, OH• is the most dominant one. The sonochemical production of hydrogen is entirely dependent on the number of hydroxyl radicals formed by acoustic cavitation. Therefore, in order to estimate the amount of hydrogen production by water sonolysis, it is essential to understand the sonochemical effect caused by ultrasonication, i.e. characterisation of the number of radicals formed by sonolysis of water.

Electrolytic hydrogen production can be enhanced by coupling ultrasound with the electrochemical cell. Ultrasonication causes degassing of the electrode surface and electrolyte, disruption of the Nernst diffusion layer, enhancement of mass transfer between electrode and electrolyte, activation and cleaning of the electrode surface during water electrolysis for hydrogen production (3). Therefore, it is also crucial to understand the enhancement of the mass transfer between electrode and electrolyte caused by ultrasonication.

In this study, chemical, the electrochemical and calorimetric method was used to understand the phenomena of both sonochemical and sonoelectrochemical production of hydrogen. Also, this preliminary study is very crucial to understand the behaviour of a sonochemical and a sonoelectrochemical reactor before moving towards the estimation of hydrogen production.

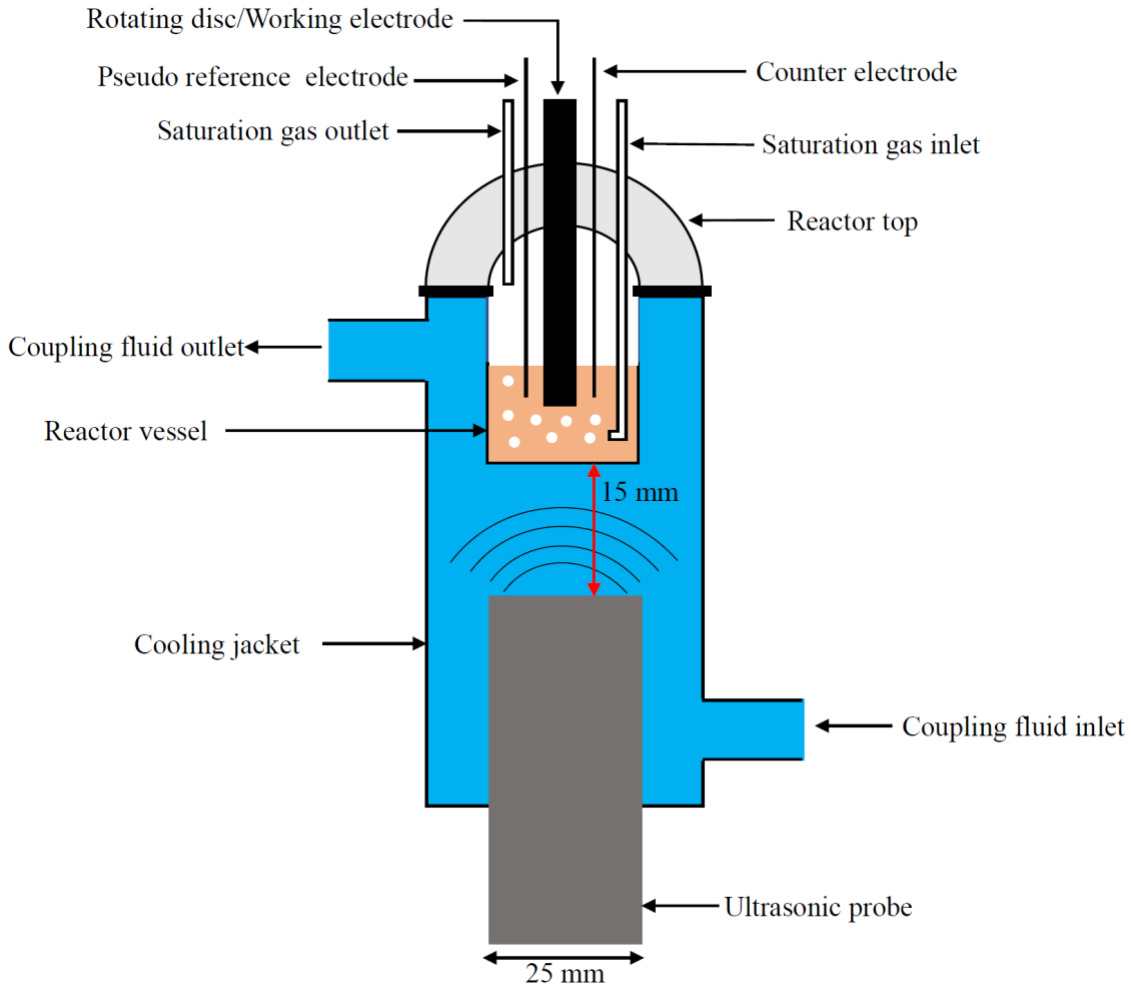

Figure 2. Schematic diagram of the microsonoreactor.

Biofuel production is also a real alternative to fossil fuels. The potential generation of energy from biological substrates has been estimated to be as high as 25% of the global energy requirements by 2035 (6), and anaerobic digestion of biomass to produce biogas is

no exception to this. The second generation of substrates for biogas is based on lignocellulosic biomasses (e.g., forestry and paper mill residues), and is currently under development. These are abundant, economical feedstocks that are not in competition with food sources (7). Despite this, there is a high lignocellulose content in such biomasses that is not easily digested anaerobically. The chemical structure of lignocellulose is exceptionally rigid and obstinate concerning its' biological degradation, meaning that the conversion of lignocellulose into usable sugars through anaerobic digestion is a slow process (8–12).

Several methods of pre-treatment have been developed to improve saccharification of feedstocks. Pre-treatment of feedstocks can be achieved in a variety of ways including enzymatic hydrolysis (13,14), acid and alkali treatments, ball milling, hot water treatment, ammonia fibre expansion, microwave irradiation, organosolv treatment and steam explosion (11,14–18). Steam explosion has evolved to become a straightforward, efficient and environmentally friendly pre-treatment of lignocellulose biomass (11,18–21). However, although the process works well on hardwoods (11,22,23), including willow (24) and birch (25), the lignocellulosic content still produces a bottle-neck in the anaerobic digestibility of such biomasses, with a significant amount of digestible components still not easily accessible. Successful attempts have been made to increase the potential for biomethane production of steam exploded birch by introducing an enzymatic step after the steam explosion (16,25); however, the potential cost of such methods at an industrial scale is not favourable.

Recent research has shown that the use of power ultrasound combined with Fenton reagents increases the saccharification of lignocellulosic-based biomass (26–28). This may provide an increase in anaerobic digestibility of lignocellulosic biomasses; however, to date, it has not been observed if power ultrasound can improve the anaerobic digestion of lignocellulosic biomass.

Methods & Materials

Reactor Design and Experimental Setup

The experimental work was carried out in two different ultrasonic frequencies of 20 kHz and 24 kHz. The 20 kHz ultrasonicator was from Sinaptec, and the 24 kHz was from Meinhardt. A double wall microreactor of 7ml was used for both transducers. A schematic diagram of the reactor is illustrated in Figure 2, and an overall experimental setup is illustrated in Figure 3.

In this setup, the transducer is situated at the bottom and is separated from the reactor volume. This kind of configuration prevents the contamination of the electrolyte by transducer erosion and ensures perfect electrical insulation of the ultrasonic transducer. The cooling fluid used in this arrangement also works as a coupling medium that allows the propagation of the ultrasonic wave from the transducer tip into the reactor solution. For the electrochemical mass transfer measurement, a variable overpressure was applied, and different coolants were used to ensure the enhanced wave propagation to the reaction medium. Two different liquids (i.e., Formulated Monoethylene Glycol (FMEG) and silicon oil (Polydimethyl siloxane, relative density 0.96 g/cm^3 and kinematic viscosity 50 cSt at 25˚C)), were used as coupling fluid.

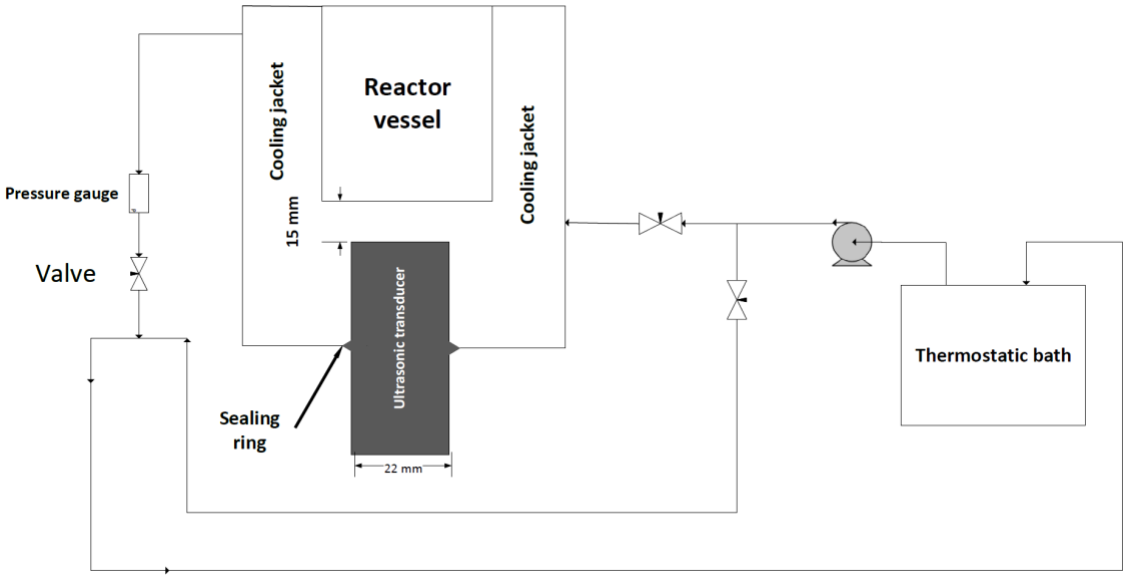

Figure 3. Schematic representation of the experimental setup.

Quantitation of Hydroxyl Radicals

Frick and Weissler dosimetry was used to study the effect that varying the reaction temperature, concentration and dissolved gases had on the reaction. For Weissler dosimetry, KI (Sigma-Aldrich) solutions of different concentrations were prepared and then 5 ml of the solution was sonicated for 5 minutes. During sonication the hydroxyl radicals react with iodide ions to form triiodide. The possible reaction pathways are illustrated in equations 3 - 6.

$$OH^{\bullet} + I^- \rightarrow OH^- + I \quad [3]$$
$$I + I^- \rightarrow I_2^- \quad [4]$$
$$2I_2^- \rightarrow I_2 + 2I^- \quad [5]$$
$$I_2 + I^- \rightarrow I_2^- \quad [6]$$

The concentration of the triiodide was then measured by UV spectroscopy at wavelength of 352 nm (The molar absorptivity, ε = 26 000 $dm^3mol^{-1}cm^{-1}$). The concentration of triiodide corresponds to the concentration of hydroxyl radicals formed by water sonolysis.

Fricke solution was prepared with the following proportions: $Fe(SO_4)_2(NH_4)_2.6H_2O$(0.25×10^{-3} mol/L), H_2SO_4 (0.4 mol/L), NaCl (1×10^{-3} mol/L) completed with ultrapure water. Before each experiments the solution was saturated using the corresponding gas for 10 minutes. The solution was then sonicated for 5 minutes. During the sonication of the Fricke solution, Fe^{2+} ions are oxidized into Fe^{3+} according to equations 7 and 8.

$$HO^{\bullet} + Fe^{2+} + H^+ \rightarrow H_2O + Fe^{3+} \quad [7]$$
$$H_2O_2 + Fe^{2+} + H^+ \rightarrow H_2O + Fe^{3+} + HO^{\bullet} \quad [8]$$

The concentration of Fe^{3+} was then measured by UV spectroscopy at 304 nm wavelength (The molar absorptivity, ε = 2197 $M^{-1}cm^{-1}$)

Mass-Transfer Measurement

The mass-transfer measurement through electrochemical method was carried out using a three-electrode assembly as illustrated in Figure 2. The working electrode was a rotating disc electrode made of platinum (d = 3 mm). The working electrode was placed in a 'face-on' geometry, where the transducer tip and the electrode were facing each other with a constant distance of 30 mm. Platinum wires of high purity were used as quasi-reference and counter electrode. Autolab PGSTAT-30 potentiostat and Autolab Rotating Disc Electrode (RDE) was used for all electrochemical measurement. Before each experiment the RDE tip was polished to mirror finish using diamond suspension of decreasing size down to 0.25 μm and also a new solution was used for each experiment.

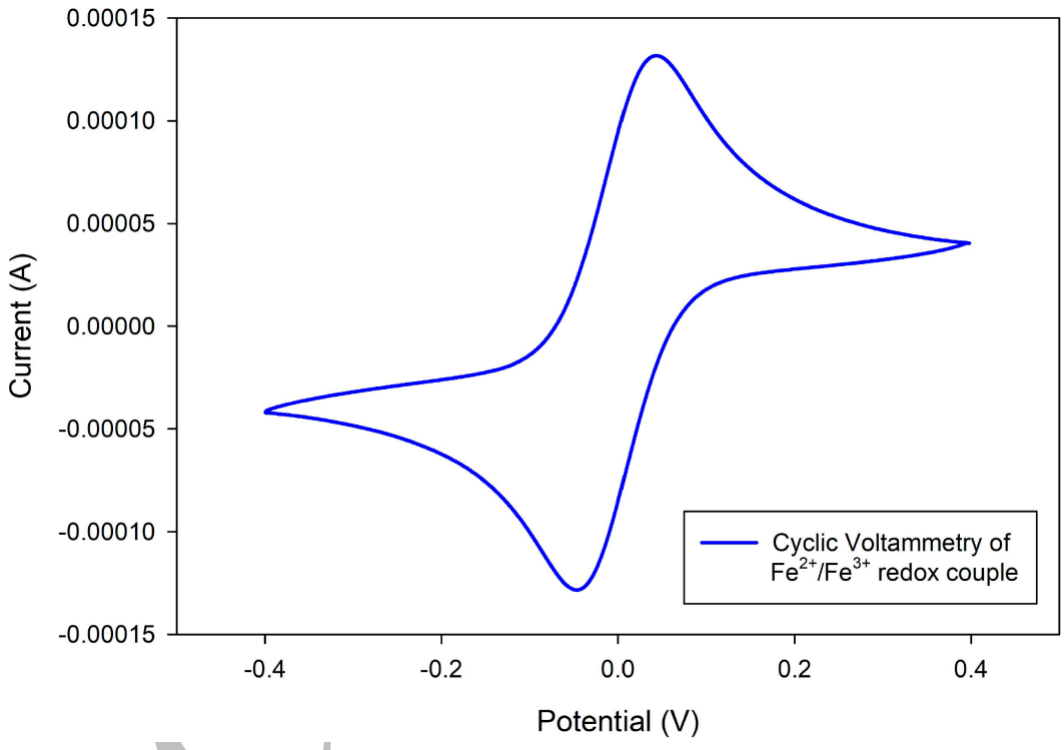

Figure 4. Typical cyclic voltammetry plot where the platinum wire was used as pseudo-reference and counter electrode, and the scan rate was 0.1 V/s.

To understand the enhanced mass-transfer phenomenon due to ultrasound, an equimolar reversible couple of Fe^{2+}/Fe^{3+} was used. The current-potential polarization curve was recorded under the steady-state conditions at 2 mV/s scan rate. Before recording the polarization curve, the cyclic voltammogram was recorded every time to be ensured that the electrochemical system (Both electrodes and the electrolytes) is functioning well. A typical voltammogram exhibiting sigmoidal shape is presented in Figure 4. The mass-transfer limited current response was decomposed into steady-state and time-dependent components (The oscillation of current signals around the average current plateau). Only steady-state current values were considered during the calculation, and the mass-transfer limited current density was calculated by taking the average of the steady-state current value. For a broader comparison, the Sherwood number was calculated from the current density, and the results were presented in Sherwood number

for better comparison. Equation 9 and 10 were used to calculate the Sherwood number (*Sh*).

$$Sh = k_d r_p / D \quad [9]$$

$$k_d = J_{lim} / nFC \quad [10]$$

Here, k_d is the mass transfer coefficient (m/s), r_p is the radius of the RDE tip, D is the diffusion coefficient (m^2/s), J_{lim} is the mass-transfer limited current density (A/m^2), n is the number of exchanged electrons, F is the Faraday number and C is the concentration of the electroactive species (29).

Calorimetric Power Measurement

For calorimetric power measurement, 5 ml of ultrapure water was sonicated for 1 minute and the rate of temperature increase due to the conversion of mechanical energy into heat was recorded in each second using a National Instruments thermocouple and by the aid of LabView software. For the acoustic power measurement without any overpressure of the coupling fluid, the inlet and outlet valves were closed, and then sonication was started for one minute. For sonication with an overpressure of the coupling fluid, the outlet valve was closed, and then the inlet valve was regulated in such a way that the desired overpressure was obtained. Then the sonication was carried out for one minute with the desired overpressure. During the sonication in the closed system of the coupling fluid, the pressure tends to rise from the desired pressure. In that case, the outlet valve was released slightly to decrease the increased pressure from the desired pressure. Finally, the calorimetric power was calculated using equation 11.

$$P = C_p \rho V (dT/dt)_{t=0} \quad [11]$$

Here, P is the acoustic power in Watt, C_p is the heat capacity of the liquid, ρ is the density of the liquid, V is the volume of the liquid and $(dT/dt)_{t=0}$ is the initial rate of temperature change. The slope of the time-dependent temperature change shows a linear shape as expected. The calorimetric power measurement results were then presented as acoustic intensity, I_t (W/cm^2) where the acoustic power was divided with the area of the ultrasonic emitting device (sonotrode).

Birch Biomass Utilization

Birch Wood Raw Material. Birchwood (*Betula pubescens*) originated from a tree harvested in Norway. The wood was shredded into chips of around 30 mm. This was then dried at room temperature.

Steam Explosion Pre-treatment. The steam explosion pre-treatment was performed as described previously (11,19), using a steam explosion instrument designed by Cambi AS (Asker, Norway), at the Norwegian University of Life Sciences in Ås, Norway. The milled birch was added to the steam pressure with a residence time of 10 minutes. The steam-exploded birch wood was stored at -20°C before further use. The dry matter content of the steam exploded sample was 34%.

Inoculum. The microbial inoculum for the biomethane potential (BMP) experiments was obtained from the Biokraft biogas plant (Skogn, Norway), from a large-scale

continuous mesophilic anaerobic digester. Before the BMP test, the inoculum was incubated at 39°C to reduce endogenous biogas production. The inoculum was diluted to 9 g volatile solids (VS) per litre. The diluted inoculum had a pH of 7.5.

Birch Sonochemical Treatment. The power ultrasound experiments were conducted at a pH of 4 in a volume of 200 mL. The steam-exploded birch was dissolved in water at 5% wet weight (i.e., 10 g of steam exploded birch per 200 mL of water). $FeCl_3$ was added to concentrations of 0.001, 0.005. 0.1. 0.3 or 0.5 M into the water-birch mixture. Power ultrasound was performed at 24 kHz for 2 h, at 30 W using a UP200S ultrasonic transducer (Hielscher, Germany). Samples were maintained at -20°C before further use.

Fenton-Like Reaction. The samples had H_2O_2 added to a molar ratio ($FeCl_3$: H_2O_2) of 1:1 or 1:10. The reaction was maintained for 2 h.

Biomethane Potential. The processed samples were digested anaerobically in sealed batch bottles. These were performed in triplicate with inoculum and processed samples, with inoculum alone as a control batch. The bottles were flushed with nitrogen gas and closed with a rubber septum and sealed, as described by Ekstrand et al. (30). These were incubated at 39°C indefinitely with regular agitation.

Birch Wood Composition Analysis. Analysis of the dry matter (DM) and volatile solids (VS) was performed on the steam exploded birch wood and inoculum using standard methods (31). The dry matter was determined by incubation of the birch wood and inoculum at 105°C for 24 h. The mass of the samples after the incubation was compared to the mass pre-incubation to acquire a percentage of DM. Samples were then incubated at 550°C for 4 hours in a muffle furnace. The weight of the samples after incubation in the muffle furnace was compared to the weight of the sample before incubation to acquire a percentage of VS.

Gas Production Volume. Measurement of the produced gas volume was achieved using an optimised liquid displacement method. The volume of gas was then adjusted for temperature using Charles´s law.

Gas Composition Analysis. Regular 10 mL samples of gas from each experiment was extracted for compositional analysis. The composition was analysed using gas chromatography (SRI 8610C, SRI Instruments, USA), equipped with a thermal conductivity detector using hydrogen as the carrier gas. A standard mixture of CO_2, CH_4, H_2 and N_2 was used as a calibrating gas. Using the volume of gas calculated with the liquid displacement method, and the percentage of methane present in the samples, methane production was calculated for the experiments. All methane production levels are the average of 3 separate experiments and have been corrected by subtracting the endogenous methane production levels for the inoculum only experiments.

Results and Discussion

Transmission of Ultrasonic Energy from One Medium to Another

Due to the unique configuration of the microsonoreactor (Figure 2), it is always challenging to transmit the ultrasonic energy from the cooling jacket into the reactor

since the maximum amount of energy is dissipated in the cooling/coupling media. This energy is lost due to the cavitation occurred in the coupling fluid. If by any means it would be possible to stop the cavitation in the coupling fluid, then it would be possible to transfer the highest amount of acoustic energy from the coupling fluid into the reactor.

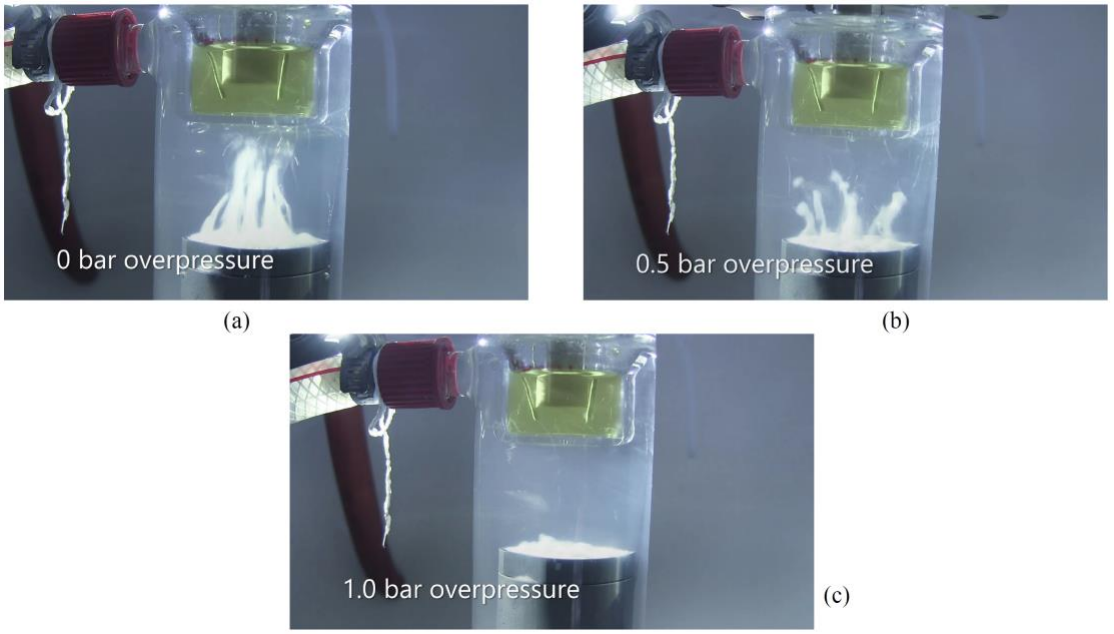

Figure 5. Effect of overpressure on the cavitation activity of silicon oil where different overpressures were applied in the silicon oil. Here silicon oil works both as cooling and coupling media for ultrasonic wave propagation (a) 0 bar overpressure in the coupling fluid, (b) 0.5 bar overpressure and (c) 1.0 bar overpressure

There are two possible ways to damping the cavitation phenomenon in the coupling fluid. One way is to increase the pressure of the coupling fluid higher than the cavitation threshold or acoustic pressure. In this concept, the ultrasonic wave travels through a high-pressure zone (Coupling medium) into an atmospheric pressure zone (reactor volume). The cavitation activity is dampened in the high-pressure zone during the propagation of the ultrasonic wave and cavitates in the atmospheric pressure zone. Another way is to use a fluid that does not cavitate but allows the propagation of ultrasonic wave from the coupling media into the reactor volume. One must be very careful when choosing a non-cavitating fluid. The fluid must be non-degradable by the violent ultrasonic vibration, non-toxic, non-flammable and above all, non-cavitating. It is quite challenging to find this kind of fluid that meets all the requirements. One possible candidate is silicon oil.

In this work formulated monoethylene glycol (FMEG) was used as the initial coupling/cooling fluid. Then the fluid circulation line was cleaned and dried, and silicon oil was used instead of FMEG. The cavitation phenomena in silicon oil are presented in Figure 5. The silicone oil is not entirely a non-cavitating fluid. Without overpressure (Figure 5a), the silicon oil cavitates moderately. Once the pressure is increased from 0 bar to 0.5 bar, the cavitation activity starts to decrease, and at 1.0 bar the cavitation is entirely damped. Therefore, it is clear that at 1 bar of overpressure the silicon oil act like a non-cavitating liquid which ensures the maximum amount of energy transfer from the coupling medium into the reactor volume. As can be seen from Figure 6, the transmission of ultrasonic energy through the silicon oil is more than double that of the FMEG. For FMEG, the increase of acoustic energy with increasing overpressure is insignificant. However, for silicon oil, at 0 bar overpressure, the acoustic intensity is 2.7 W/cm2,

whereas at 1 bar the acoustic intensity is 4.5 W/cm2. This clearly shows the damping of cavitation in the coupling fluid and increased cavitation activity in the reactor volume. This increased cavitation activity will increase the overall sonochemical efficiency of the reactor and will enhance hydrogen production both sonochemically and sonoelectrochemically.

Characterization of Hydroxyl Radicals

The acoustic intensity measurements were supplemented by the sonochemical reactivity studies where both Fricke and Weissler dosimetry methods were compared. It was observed that with increasing overpressure, the absorbance for both triiodide and ferric ions were increased. Formation of hydroxyl radicals depends on the nature of cavitation bubbles: transient (or inertial bubble) and stable (non-inertial) cavitation bubbles. The stable cavitation bubbles are a repetitive transient bubble, which nearly collapses and grows several times. This repetitive behaviour can last for several days. On the other hand, the transient cavitation bubble has a much shorter life span and collapses violently only after few acoustic cycles.

Sonochemical reactions or radicals are formed only during the collapse of the transient cavitation bubble, whereas the stable cavitation bubble does not have any sonochemical effect during a collapse. For indirect sonication (Figure 2), it was observed that without overpressure, only stable cavitation bubbles are present in the reactor volume. This phenomenon was observed when an aluminium foil was submerged in the reactor solution. After a few minutes of sonication, many holes were observed on the aluminium foil, which was caused by the strike of a stable cavitation bubble. However, at 0 overpressure, no or minimal formation of hydroxyl radicals was observed (Figure 7).

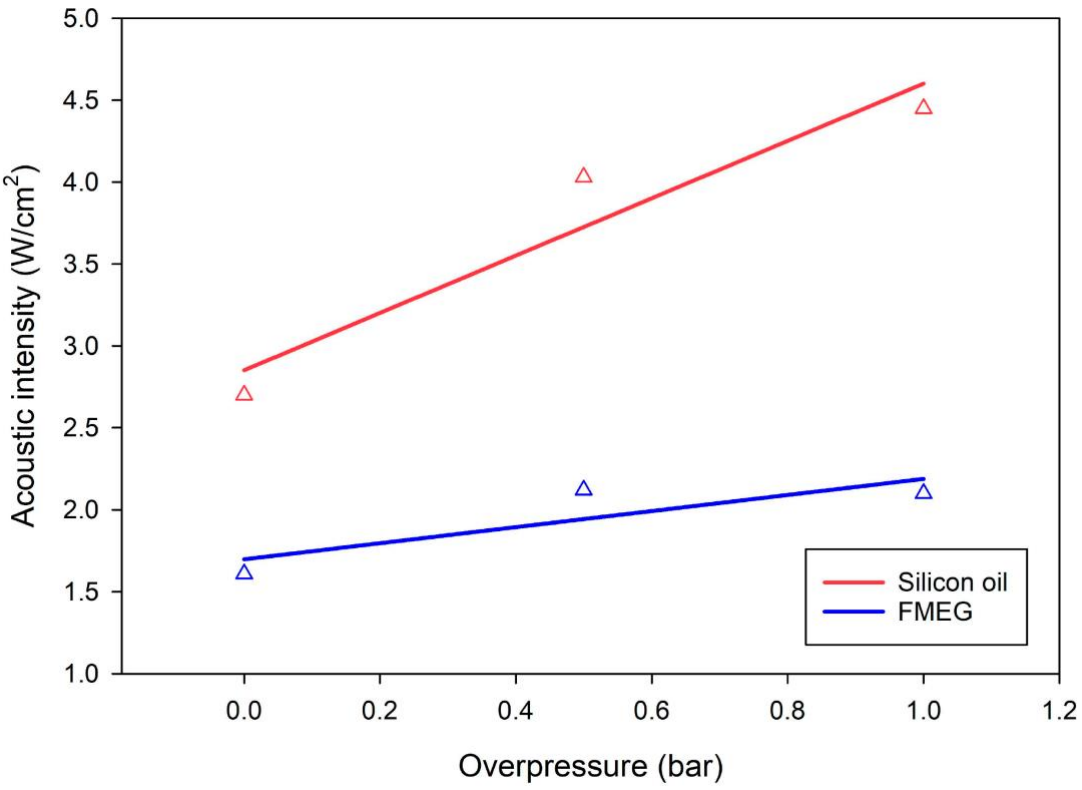

Figure 6. Acoustic intensity as a function of overpressure of the different coupling fluid.

This proves that at 0 overpressure, we almost have no sonochemical activity inside the reactor volume. Once the coupling fluid pressure was increased from 0 bar to 0.5, an apparent increase of sonochemical activity was observed meaning that transient cavitation bubbles are formed inside the reactor volume, which violently collapse and produces radicals. Increasing overpressure also increases the production of radicals, which can be seen from both Fricke and Weissler dosimetry methods. The more the formation of hydroxyl radicals is, the more the production of hydrogen gas since the hydrogen gas production through sonochemical methods is the radical's recombination reactions (equation 1 and 2). Also, using silicon oil as coupling fluid instead of water or FMEG will significantly increase the sonochemical activity in the reactor since silicon oil enhances higher transmission of acoustic energy by damping the cavitation activity in the coupling area.

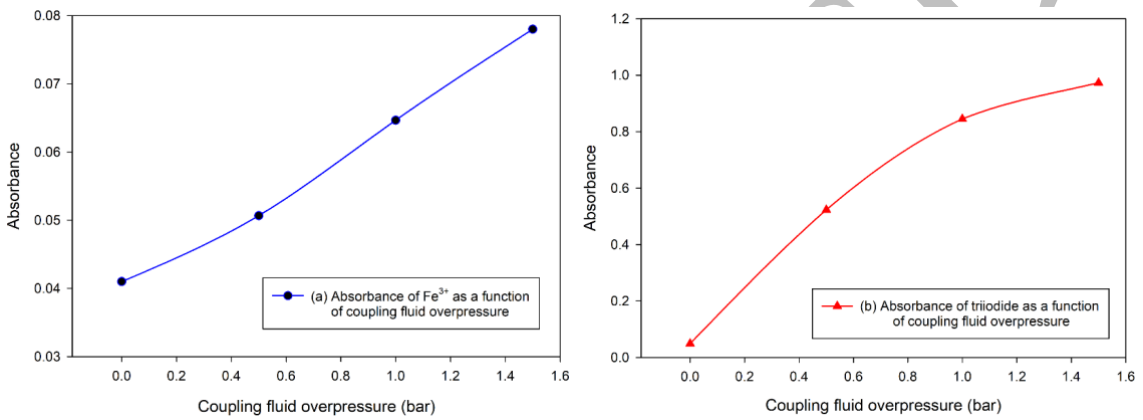

Figure 7. Effect of overpressure on hydroxyl radical formation in the presence of air at 10 ℃ (a) Fricke dosimetry, (b) Weissler dosimetry.

Mass-Transfer Enhancement

Mass-transfer measurements were carried out in three different overpressure (0 bar, 0.5 bar and 1.0 bar overpressure) and using both FMEG and silicon oil as coupling fluid. The current-potential polarisation curves under steady-state conditions are presented in Figure 8 at a different overpressure with silicon oil as the coupling fluid. It can be seen that at 0 and 0.5 bar overpressure the steady-state current response is almost similar. However, at 1 bar of overpressure, we witnessed a very high current response and oscillations. The oscillations on the signal plateau correspond to cavitation activity. The higher oscillation means higher cavitation activity as well as higher mass/electron transfer between electrode and electrolytes. These highly oscillated signal plateaus are also representative of the phenomena observed in Figure 5. At 1 bar, the cavitation activity was almost damped in the silicon oil and high cavitation activity was observed in the reactor volume. This phenomenon is also representative for the case of acoustic power (Figure 6) where at 1 bar, we witnessed very high acoustic power due to elevated cavitation activity.

The mass-transfer limited current densities were also plotted in terms of dimensionless Sherwood number with different overpressure for silicon oil and then the results were compared with the literature. Figure 9 represents the *Sh* number at a different overpressure of silicon oil with increasing ultrasonic amplitude. The higher the ultrasonic amplitude is, the higher the electric energy converted into acoustic energy. As can be

seen from Figure 9, the Sh number at 0 and 0.5 bar overpressure are similar meaning that the cavitation activity is similar in these two conditions. However, at 1 bar, the Sh number is four times higher than at 0 or 0.5 bar overpressure. Also, the increase in amplitude is very significant for 1 bar of overpressure. Comparing with literature (29), the obtained Sherwood number with silicon oil is also four times higher at 1 bar than what was obtained with FMEG as a coupling fluid.

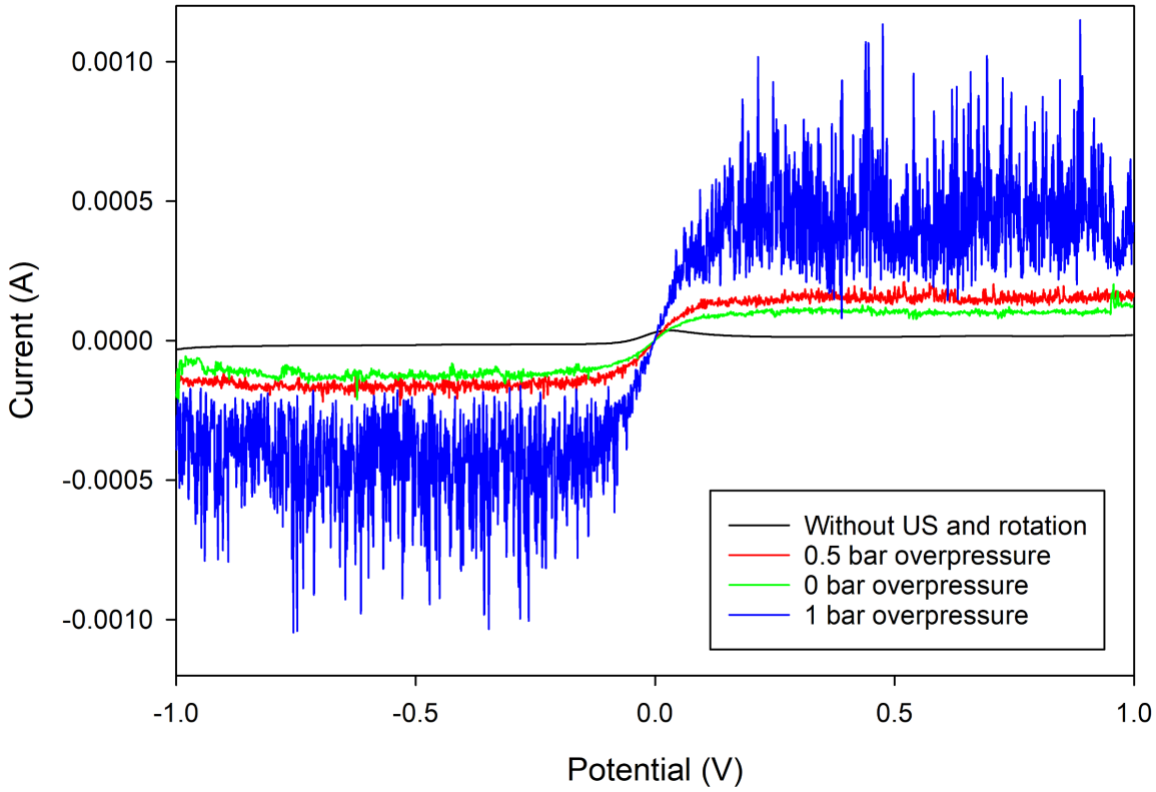

Figure 8. Current-potential polarisation curves of the Fe^{3+}/Fe^{2+} reversible couple under steady-state conditions at a different overpressure of coupling fluid. Here Pt rod was used as a pseudo-reference and counter electrode.

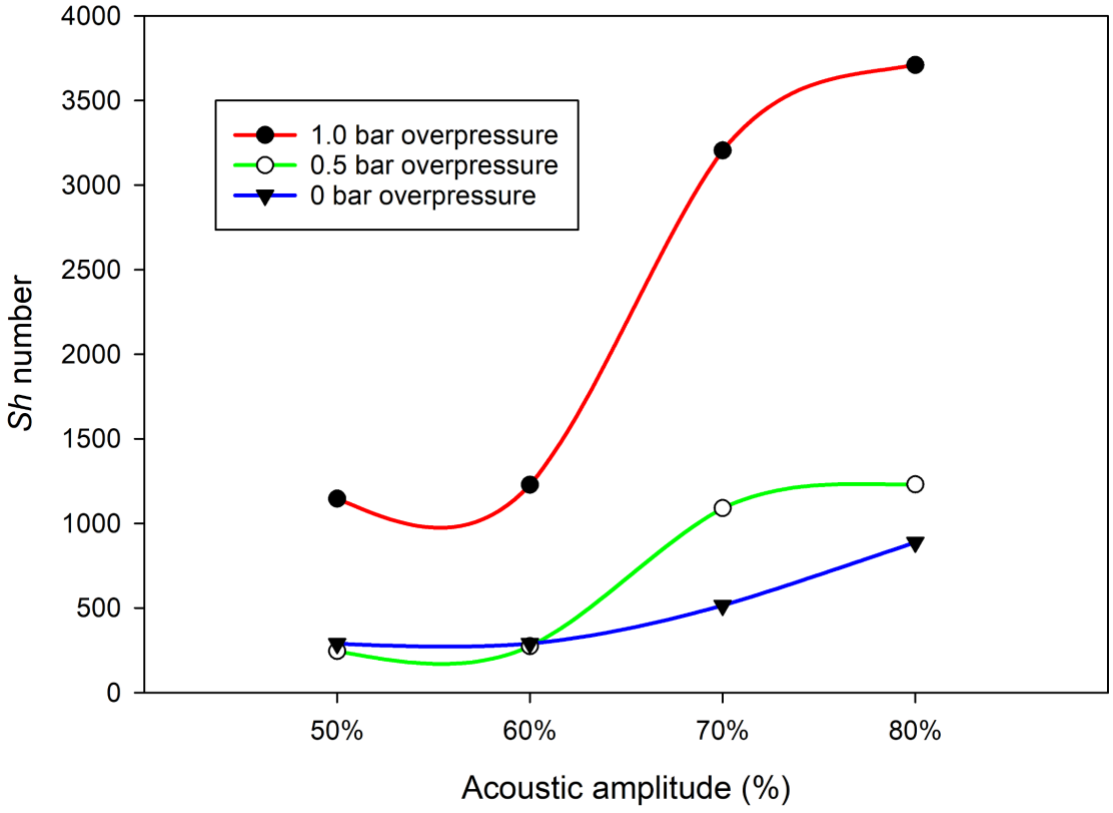

Figure 9. Sherwood number at a different overpressure of silicon oil with increasing acoustic amplitude.

These higher Sh number is very significant when it comes to electrochemical production of hydrogen. Using silicon oil as a coupling fluid at 1 bar overpressure will significantly improve the hydrogen evolution reaction at the cathode due to the very high mass-transfer between electrode and electrolyte. Consequently, the improved hydrogen evolution reaction will increase the overall production of hydrogen through the sonochemical and sonoelectrochemical method simultaneously and separately. This improved mass-transfer can be useful not only for hydrogen production but also any other electrochemical process for fuel productions.

Birch Wood Treatment with Power Ultrasound and Fenton-Like Reagents

Steam exploded birch wood was dissolved in water as described previously. The $FeCl_3$ was then added to the dissolved steam-exploded birch wood to concentrations between 0 – 0.01 M, as outlined in Table 1. The pH was adjusted to 4 before power ultrasound to optimise the degradation of lignocellulosic biomass by the Fenton reaction that will occur with the H_2O_2 produced by the ultra-sonification process (27). Power ultrasound was applied to the mixture at a power of 30 W and a frequency of 24 kHz for a period of 2 h. After the power ultrasound process was complete, the addition of H_2O_2 to some of the samples was made at the concentrations outlined in Table 1 to initiate the Fenton reaction for a period of 2 h. BMP tests by anaerobic digestion of these processed birch samples were then performed. A control test was also included that had no power ultrasound, or Fenton reaction treatments applied.

TABLE I. Sonochemistry and Fenton-Like Reagent Reaction Specifications.

Experiment	[$FeCl_3$] (M)	[H_2O_2] (M)	Power ultrasound duration (h)
Control	0	0	0
1	0	0	2
2	0.05	0	2
3	0.001	0.01	0
4	0.001	0.01	2
5	0.001	0.001	2

Biogas Production Rate. In terms of an industrial biogas production plant, the rate of biogas evolution is an essential variable because an increased rate will lead to a decreased retention time, allowing for an increased plant capacity without expansion of the existing plant infrastructure. The maximum rate of biogas production is calculated by determining the production of biogas per day during the exponential phase of anaerobic digestion. The rate of biogas production was reduced by power ultrasound and Fenton reaction treatments compared to the control when applied individually, as shown by experiments 1 – 3 (Table 2). However, when the power ultrasound and Fenton reaction treatments of the lignocellulosic biomass were both applied to the sample, the rate of biogas production increased compared to the control (experiment 4).

TABLE II. Biogas Production Rate During Exponential Phase.

Experiment	Maximum Rate (mL/gVS7day)
Control	72.11
1	41.32
2	54.87
3	43.37
4	74.40
5	77.26

Furthermore, a 10-fold reduction of the H_2O_2 concentration used for the Fenton reaction increased the rate of biogas production further (experiment 5). This increase in rate would allow for a shorter retention time of the biomass substrate in an anaerobic digestor, reaching the maximum BMP faster. In the context of a continuously fed industrial anaerobic digestor, this will increase the overall biogas capacity of the plant without increasing the size of the anaerobic digester.

Concluding Remarks

The power ultrasound area of research already covers various studies from organic syntheses, polymeric materials syntheses, production of nanomaterials, environmental (soil and water) treatments, water disinfection, corrosion of metals, analytical procedures, film and membrane preparations to the elucidation of electrochemical mechanisms in various ‘exotic’ solvents. Here, the utilisation of power ultrasound for the production of biogas and H_2 has been explored. Power ultrasound has been observed to be a tool that can allow for more intensive and more efficient ways for the energy conversion required within the production of H_2 and biogas. This research on power ultrasound applications in a renewable energy context may open pathways for future industrial production of H_2 and biogas, allowing further utilisation of non-fossil fuel alternatives in our society.

Acknowledgements

The authors would like to acknowledge the support from the ENERSENSE research initiative at NTNU.

References

1. B. Pollet, *Power ultrasound in electrochemistry: from versatile laboratory tool to engineering solution*, (2012).
2. B. G. Pollet, *Electrochem. Soc. Interface*, **27**, 41–42 (2018).
3. M. H. Islam, O. S. Burheim, and B. G. Pollet, *Ultrason. Sonochem.*, **51**, 533–555 (2019).
4. O. S. Burheim, *Engineering energy storage*, Academic Press, (2017).
5. S. Merouani, O. Hamdaoui, Y. Rezgui, and M. Guemini, *Ultrason. Sonochem.*, **22**, 41–50 (2015).
6. H. Kopetz, *Nature*, **494**, 29–31 (2013).
7. M. Balat and H. Balat, *Appl. Energy*, **86**, 2273–2282 (2009).
8. S. J. Horn, G. Vaaje-Kolstad, B. Westereng, and V. Eijsink, *Biotechnol. Biofuels*, **5**, 45 (2012).
9. R. J. Quinlan et al., *Proc. Natl. Acad. Sci.*, **108**, 15079–15084 (2011).
10. G. Vaaje-Kolstad et al., *Science (80-.).*, **330**, 219–222 (2010).
11. V. Vivekanand, E. F. Olsen, V. G. H. Eijsink, and S. J. Horn, *Bioresour. Technol.*, **127**, 343–349 (2013).
12. S. Sarker, J. J. Lamb, D. R. Hjelme, and K. M. Lien, *Appl. Sci.*, **9**, 1915 (2019).
13. J. J. Lamb, S. Sarker, D. R. Hjelme, and K. M. Lien, *Adv. Microbiol.*, **8**, 378 (2018).
14. J. J. Lamb, D. R. Hjelme, and K. M. Lien, *Adv. Microbiol.*, **9**, 359–371 (2019).
15. J. J. Lamb, M. H. Islam, D. R. Hjelme, B. G. Pollet, and K. M. Lien, *Ultrason. Sonochem.*, 104675 (2019) http://www.sciencedirect.com/science/article/pii/S1350417719308909.
16. P. W. Harris and B. K. McCabe, *Appl. Energy*, **155**, 560–575 (2015).
17. P. Kumar, D. M. Barrett, M. J. Delwiche, and P. Stroeve, *Ind. Eng. Chem. Res.*, **48**, 3713–3729 (2009).
18. L. P. Ramos, *Quim. Nova*, **26**, 863–871 (2003).
19. S. J. Horn, Q. D. Nguyen, B. Westereng, P. J. Nilsen, and V. G. H. Eijsink, *Biomass and Bioenergy*, **35**, 4879–4886 (2011).
20. D. C. Kalyani, M. Zamanzadeh, G. Müller, and S. J. Horn, *Appl. Energy*, **193**, 210–219 (2017).
21. W. Jin et al., *Appl. Energy*, **175**, 82–90 (2016).
22. S. J. Horn and V. G. H. Eijsink, *Biosci. Biotechnol. Biochem.*, **74**, 1157–1163 (2010).
23. P. Sassner, M. Galbe, and G. Zacchi, in *Applied Biochemistry and Biotechnology - Part A Enzyme Engineering and Biotechnology*,, vol. 124, p. 1101–1117, Humana Press, Totowa, NJ (2005).
24. J. H. Svein, M. E. Maria, K. N. Henrik, L. Roar, and G. H. E. Vincent, *Bioresour. Technol.*, **102**, 7932–7936 (2011).
25. V. Vivekanand, E. F. Olsen, V. G. H. Eijsink, and S. J. Horn, *13th World Congr. Anaerob. Dig.*, 7936 (2013).
26. S. Wang, X. Ouyang, W. Wang, Q. Yuan, and A. Yan, *RSC Adv.*, **6**, 76848–76854 (2016).

27. T. Sheng, L. Zhao, W.-Z. Liu, L. Gao, and A.-J. Wang, *RSC Adv.*, **7**, 32076–32086 (2017).
28. V. P. Bhange et al., *J. Environ. Heal. Sci. Eng.*, **13**, 12 (2015).
29. C. Costa et al., *Phys. Chem. Chem. Phys.*, **10**, 2149–2158 (2008).
30. E.-M. Ekstrand et al., *Appl. Energy*, **112**, 507–517 (2013).
31. A. P. H. Association, A. W. W. Association, W. P. C. Federation, and W. E. Federation, *Standard methods for the examination of water and wastewater*, American Public Health Association., (1915).